

Controlled, Stepwise Syntheses of Oligomers with Modified Quinoxaline Backbones

Jerome Klein,^[a] Nicole Jung,^{*[a, b]} and Stefan Bräse^{*[a, b]}

New oligomers based on quinoxaline units were successfully synthesized through multistep reactions using Wittig coupling, affording (*E*)-(quinoxalin-2-yl)ethene oligomers. Diverse quinoxaline-based phosphonium salts were designed and synthesized, enabling versatility and compatibility regarding the

oligomer-building process. The characterization of the oligomers showed excellent stereoisomer specificity, i.e., a fully *E*-configured conjugated π -system. The oligomers' light absorption/emission profiles indicate potential properties for an application in materials science.

Introduction

Quinoxalines and quinoxalinones are closely related and interconvertible molecule classes with potential applications in synthetic chemistry,^[1] biology,^[2–6] and materials science.^[7] Due to their multifaceted electronic and structural features, quinoxalines have been target compounds in various studies over the past years, aiming to improve the properties of materials used for organic semiconductors,^[8,9] battery electrodes,^[10] or OLED (organic light-emitting diode) components.^[11] Furthermore, quinoxalines were used as a core structure to synthesize polymers and oligomers (Figure 1) in the past.^[12–15] The formation of these higher molecular structures were usually based on polymerization synthesis involving Grignard (Figure 1b),^[12–14] nickel-,^[13] or palladium-catalyzed (Figure 1a and 1c) reactions.^[12,13,15,16] The currently known reactions allow the formation of molecules with diverse sizes as polymers, containing a moderate amount of units (4–6 units) to a high degree of polymerization (up to 300 units). Nevertheless, the resulting molecules consist of only one specific quinoxaline building block. Therefore, these processes show synthetic limitations such as lower functionalization ability or/and less growth control. Polymerization reactions do not enable size-specific molecules; only a repartition of various lengths can be generated. However, non-quinoxaline-based approaches re-

cently demonstrated the regio- and sequence-defined oligomer synthesis, allowing the synthesis of new polymers with absolute control over chain length, sequence, and topology.^[17]

Literature-known procedures reported alkene bridges between quinoxalines,^[18] between quinoxaline and benzene (Figure 1d),^[19] or even between quinoxaline and carbazole within polymerization reactions or dimerization.^[20] The method allowing the longest oligomer was based on the Wittig coupling of terephthalaldehyde or carbazole-3,6-dicarbaldehyde derivatives with quinoxaline-based phosphonium salts.^[19,20] This process was successfully applied to synthesize oligomers with a moderate number of units (~8 and ~16 units with benzene and carbazole, respectively).

This work aims for the controlled synthesis of quinoxaline-based oligomers, enabling further investigations of the properties and potential applications of this interesting compound class. While the direct connection of quinoxaline building blocks has been explored in several other studies before, C=C double-bond connected purely quinoxaline-based oligomers are unknown to the best of our knowledge, and their potential is still unexplored. Furthermore, the alkene-linkage of monomers through consecutive Wittig couplings offers a highly versatile method for oligomer synthesis.

Results

Synthetic procedure

The controlled synthesis of oligomeric structures based on quinoxalines, as envisaged in this study, is described in Figure 2. We aimed for a feasible approach to form structures such as tail-X-X-X-X (Figure 2a) via consecutive repetitions of Wittig reactions using different quinoxaline-based phosphonium salt building blocks 1–4 (Figure 2c). The planned synthesis strategy includes the installation of a tail on the first quinoxaline building block (Figure 1b, structure A-1), its oxidation to an aldehyde (A-1→A-1*), and subsequent Wittig reaction with a phosphonium salt building block such as 1. The resulting “2-mer” (A-1-1) can then again be oxidized (A-1-1→A-1-1*), being prepared for the next step of a chain elongation via Wittig

[a] Dr. J. Klein, Dr. N. Jung, Prof. Dr. S. Bräse
Institute of Biological and Chemical Systems (IBCS-FMS),
Karlsruhe Institute of Technology
Hermann-von-Helmholtz-Platz 1
76344 Eggenstein-Leopoldshafen (Germany)
E-mail: Nicole.jung@kit.edu
braese@kit.edu

[b] Dr. N. Jung, Prof. Dr. S. Bräse
Institute of Organic Chemistry,
Karlsruhe Institute of Technology
Hermann-von-Helmholtz-Platz 1
76344 Eggenstein-Leopoldshafen (Germany)

Supporting information for this article is available on the WWW under <https://doi.org/10.1002/ejoc.202200764>

© 2023 The Authors. European Journal of Organic Chemistry published by Wiley-VCH GmbH. This is an open access article under the terms of the Creative Commons Attribution License, which permits use, distribution and reproduction in any medium, provided the original work is properly cited.

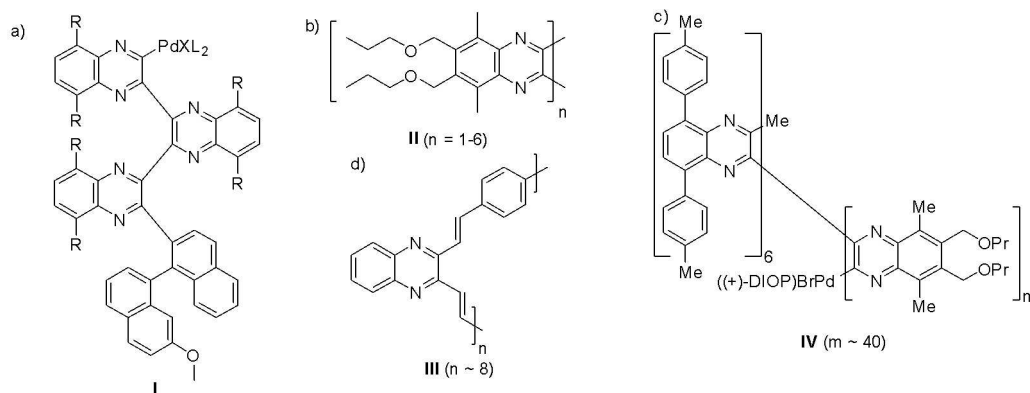


Figure 1. Literature-known oligomers and polymers consisting of quinoxaline units were gained using either palladium-catalyzed reactions (a, c), Grignard reaction (b), or Wittig coupling (d).^[12,13,16,19]

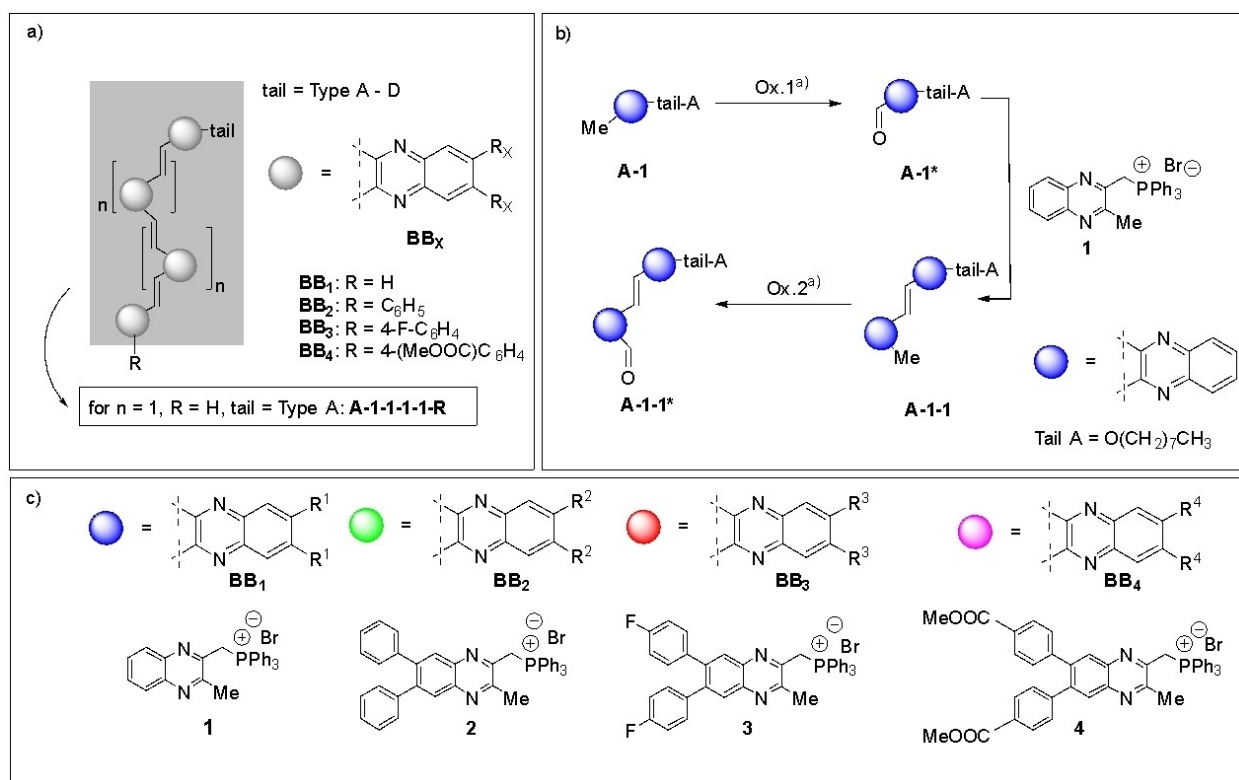


Figure 2. Schematic representation of the aims of this study: (a) General structure of the oligomer target consisting of different quinoxaline blocks. See the Supporting Information (synthesis section) for a detailed drawing of the structures; (b) strategy for the controlled stepwise formation of oligomers, described with tails of type A and building block **BB1** yielding the coupling of two quinoxaline units (= "dimer"), (c) structures of the Wittig salt building blocks used in this study.

coupling. The oligomers can be built with four different building blocks (BB) (**BB1–BB4**, corresponding to labels 1–4 in the final oligomer), each allowing diversity to be introduced in the final overall sequence. Altogether, the synthesis strategy requires four different processes: 1) the attachment of the tail to the first monomer, 2) the oxidation of the methyl groups to aldehydes, 3) the reaction of the phosphonium salt 1–4 with the previously synthesized aldehyde via Wittig coupling to gain the desired C=C connectivity, 4) another oxidation of the

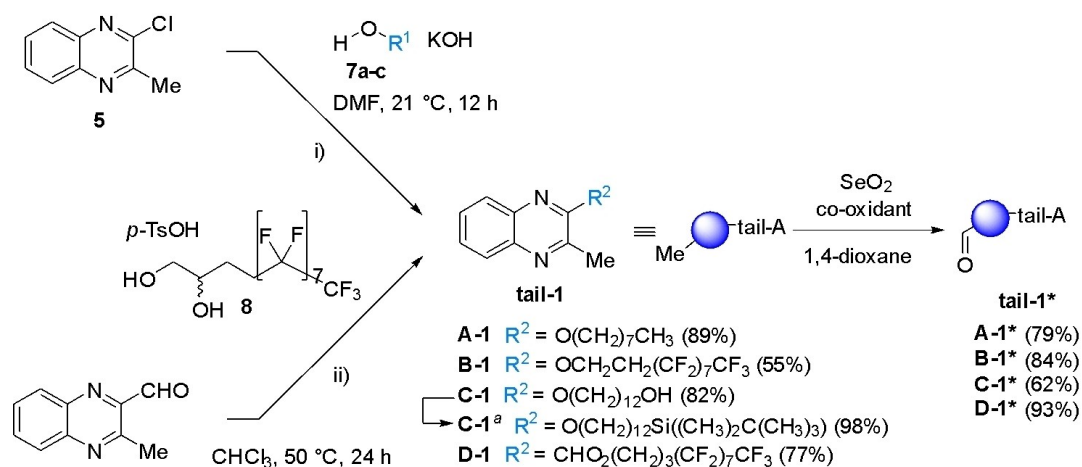
methyl group to repeat the Wittig coupling. The initial and final monomers have a special role in the reaction sequence as they can have additional functions in the pyrazine part of the quinoxaline. Here, combinations with various tail structures or terminal substituents are possible. Modifications in the benzene part of the quinoxaline (R^1 – R^4 in Figure 1, from here on called the backbone) and the tail structures were used in this study to adapt the properties of the oligomers.

For a variation of the first element in the oligomer synthesis, four tails of different lengths and chemical compositions were selected to be attached to quinoxaline monomers (A-1 to D-1, Scheme 1). All alkyl tails, each consisting of an aliphatic chain of at least eight carbons, were installed to modulate, in particular, the solubility properties of the final oligomers. The use of perfluorinated tails (type B and D) should demonstrate, in addition, the installation of functional tails for improved purification options via fluororous solid-phase extraction (F-SPE) applied to some intermediates (see Supplemental Information).^[21] The attachment of tails of type A-D was reached in two different ways. To gain A-1 to C-1, 2-chloro-3-methylquinoxaline (5) was converted with perfluorinated 7b or aliphatic alcohols 7a and 7c (Scheme 1). The TBDMS (*tert*-butyldimethylsilyl) protecting group was incorporated into C-1 to avoid undesired side reactions (Supplemental Information Scheme S4). Building block D-1 was synthesized by condensing 3-methylquinoxaline-2-carbaldehyde (6) and the perfluorinated diol 8 to an acetal (Scheme 1). The resulting protocol described in Scheme 1 results from an optimization of the nucleophilic reaction with different bases (see Supplemental Information (Scheme S3 and Table S1)). The next step of the synthetic process was the oxidation of the methyl group at the quinoxaline core to form an aldehyde as functionality to realize another Wittig coupling. According to similar reactions in the literature,^[22] SeO₂ was used as an oxidant, and *tert*-butylhydroperoxide as a co-oxidant (Scheme 1). The optimization of the oxidation process can be found in the Supplemental Information (Scheme S5 and Table S2).

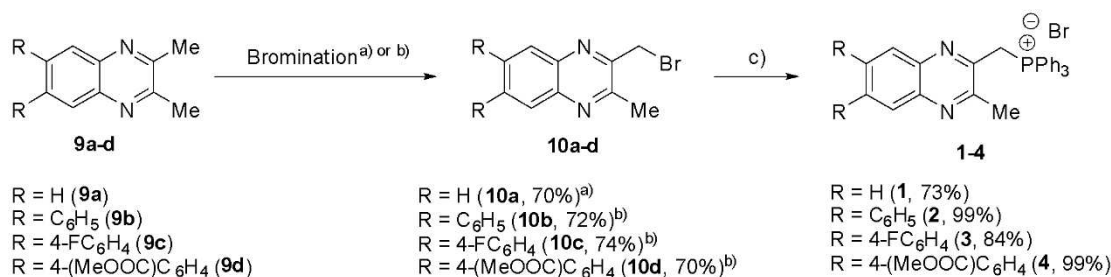
After the successful synthesis of aldehydes A-1* to D-1* available for oligomer synthesis, suitable triphenylphosphonium salts were prepared for the Wittig reaction as part of the envisioned elongation process. All quinoxaline-based phosphonium salts were obtained in four steps from *o*-phenylenediamine and 4,5-dibromobenzene-1,2-diamine, synthesized according to a literature procedure (Supporting Information,

Scheme S6).^[22] In the first step, the quinoxaline backbone was modified by the transformation of 4,5-dibromobenzene-1,2-diamine with three boronic acids under Suzuki coupling conditions (Supporting Information, Scheme S7). The resulting *o*-phenylenediamine derivatives afforded 2,3-dimethylquinoxalines 9a-d after condensation with butan-2,3-dione (Supporting Information, Scheme S8). These were successively subjected to bromination to yield the 2-(bromomethyl)quinoxalines 10a-d (Scheme 2). Depending on the electronic properties of the quinoxalines 9a-d, different bromination reagents were used to synthesize compounds 10. In the case of unsubstituted 2,3-dimethylquinoxaline (9a), *N*-bromosuccinimide was sufficiently reactive, even if a portion-wise addition of *N*-bromosuccinimide was necessary to avoid a drastic drop in yield. However, as soon as an electron-withdrawing substituent, such as 4-FC₆H₄ and 4-(MeOOC)C₆H₄, was added to the backbone of the quinoxaline, molecular bromine was necessary for a successful conversion. As electron-withdrawing substituents further reduced quinoxaline's reactivity, adding more than one equivalent of molecular bromine and additional heating was necessary to gain compounds 10b-d in good yields. To obtain phosphonium salts 1-4 (Scheme 2), 2-(bromomethyl)quinoxalines 10a-d were then reacted with triphenylphosphine. To avoid dimerization and the formation of various by-products, the reaction was conducted at specific temperatures and under very slow and stepwise addition of triphenylphosphine, depending on the respective substituents on the quinoxaline backbone (cf. Supporting Information Scheme S9 and Table S4).

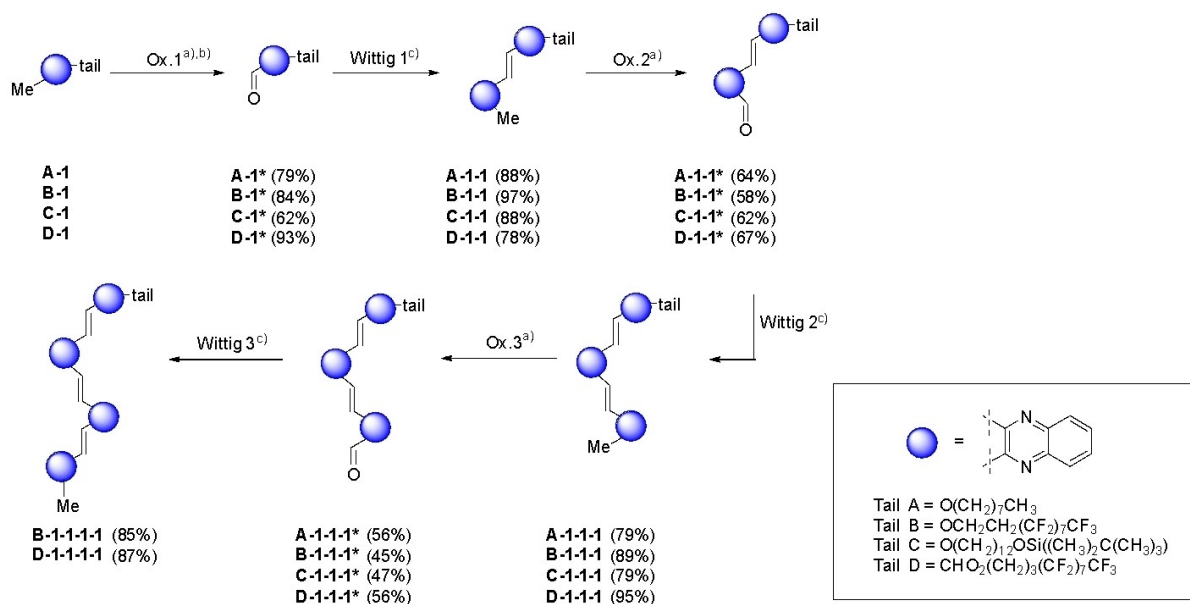
The Wittig reaction of the first monomers bearing different tails with compounds 1-4 was performed based on a literature-known procedure.^[19,20] This protocol led to very good to excellent results (usually 76 to 97%) for the reactions described in Scheme 3. Additionally, only the formation of the *E* stereoisomer was observed (Scheme S10). The *E* specificity of the oligomer has been proven by ¹H NMR (nuclear magnetic



Scheme 1. Addition of perfluoro-tails and non-perfluoro-tails to the first monomer of the oligomer synthesis. Conditions: i) KOH (1.2 equiv.), alcohol 7a-c (1.1 equiv.), DMF (*N,N*-dimethylformamide), 21 °C, 12 h; ii) *p*-TsOH (10 equiv.), diol 8 (1.1 equiv.), CHCl₃, 50 °C, 12 h; [a] Conditions: *tert*-butyldimethylsilyl chloride (TBDMSCl, 1.1 equiv.), imidazole (1.1 equiv.), 21 °C, 12 h, DMF.



Scheme 2. Synthesis of ((3-methylquinoxalin-2-yl)methyl)triphenylphosphonium bromides **1–4** starting from 2-methylquinoxaline derivatives **9a–d**. [a] Conditions: N-bromosuccinimide (1.6 equiv.), (PhCOO)₂ (0.25 equiv.), acetonitrile, 95 °C, 7 h; [b] Conditions: Br₂ (1.1 to 1.5 equiv.), DCM (dichloromethane) or CHCl₃, 0 °C or 70 °C, 2 to 12 h; [c] Conditions: PPh₃ (5.0 equiv.), DCM, –78 °C to 21 °C, 12 h.



Scheme 3. Oligomerization process using compound **1**. [a] Conditions: SeO₂ (2.0 to 5.0 equiv.), 1,4-dioxane, 50 °C to 80 °C, 12 h; [b] *tert*-butyl hydroperoxide (TBHP, 1.1 equiv.); [c] Conditions: phosphonium salt **1** (1.1 to 1.5 equiv.), NaOMe (5.0 equiv.), DCM:MeOH (2:1), 50 °C, 12 h.

resonance) spectroscopy of the resulting product **B-1-1**. Two second-order (doublets) signals from the –HC=CH– bridges showed coupling constants of $J=15.4$ Hz each, which fits a $^3J_{\text{trans}}$ coupling (see Supporting Information Figure S1). The observed stereospecificity can be explained by a steric hindrance from both quinoxalines during reaction intermediate formation and the electrical properties of the in situ generated ylide (stabilized ylide), naturally leading to *E* configurations. To determine the maximum number of oligomerization steps that can be conducted consecutively, several repetitions of oxidation and Wittig coupling process were performed using the building block of type **BB1** in combination with different tails. After attaching the next quinoxaline monomer to the compounds **A-1*** to **D-1*** (to give **A-1-1** to **D-1-1**), oxidation of the terminal methyl group (**tail-1-1**→**tail-1-1***) proceeded much slower and required elevated reaction temperatures of 60 °C or even 100 °C to give satisfying yields. Compared to the oxidation of the initial module (**tail-1**→**tail-1***), the second and third oxidation steps show each a clear

drop in yield (Scheme 3). With reaction temperatures higher than 60 °C, site-specific oxidation of the terminal methyl group was lost, and competing oxidation of the quinoxaline nitrogen occurred by the co-oxidant *tert*-butyl-hydroperoxide. Therefore, *tert*-butyl hydroperoxide was removed when oxidizing oligomers contained more than one building block. With four quinoxaline building blocks attached, the respective “tetramers” solubility became a major concern. Oligomers containing an odd number of quinoxaline building blocks showed a higher solubility in organic solvents than corresponding oligomers with an even number of quinoxaline units. For instance, the solubility of **B/D-1-1-1-1** in common organic solvents (e.g., dichloromethane, chloroform, acetone, tetrahydrofuran (THF), methanol, benzene, pyridine, DMF) was so low that NMR analysis was not possible, even at high (boiling) temperatures; therefore MALDI measurement was preferred to characterize the isolated compounds. The further extension of tetramers was, therefore, not pursued.

To introduce diversity into the target oligomers, different combinations of building blocks **BB1-BB4** were then generated based on tail-A. In the first coupling step, **A-1*** was combined with phosphonium salts **2-4** to give the dimeric compounds **A-1-2**, **A-1-3**, and **A-1-4**. All combinations were successfully gained, showing the compatibility of the strategy with different building blocks (Scheme 4, for **A-1-3** and **A-1-4**, see Supplemental Information). The dimer **A-1-2** was then used for further elongation steps, and three different trimers (**A-1-2-1**, **A-1-2-3**, and **A-1-2-4**) were investigated concerning the mutability of the building block sequence and yielded oligomers (Scheme 4). In the synthesis of the oligomer **A-1-2-4**, concurrent formation of the *Z*-isomer was observed in the last Wittig coupling if conducted at 50 °C. When carried out at 21 °C, the formation of the *Z*-isomer was not observed. In the case of **A-1-2-1** and **A-1-2-4**, oxidation according to the usual protocol yielded the respective aldehydes in 52–58% yield. For **A-1-2-3**, however, the tested oxidation conditions failed as no conversion of the oligomer, and only decomposition was observed.

Knowing that the **tail-X-X-X*** were the last soluble oligomers reachable by this process, we envisioned to couple two of these trimers to each other to maximize the extension of the oligomeric π system. Using (1,4-phenylenebis(methylene))bis(triphenylphosphonium) bromide (**11**) as a linking agent,^[24] lead to the formation of four different 3+3 oligomers, comprising a **tail-X-X-X-s-X-X-tail** structure with *para*-phenylene as a spacer (abbreviated as *s*, see Scheme 5).

All 3+3 oligomers were obtained in excellent yields following the usual protocol for Wittig coupling. As expected, the obtained 3+3 oligomers have solubility properties similar to the tetramers. However, their solubility is slightly improved - probably due to the presence of two tails - enabling us to approve the results by NMR spectroscopy.

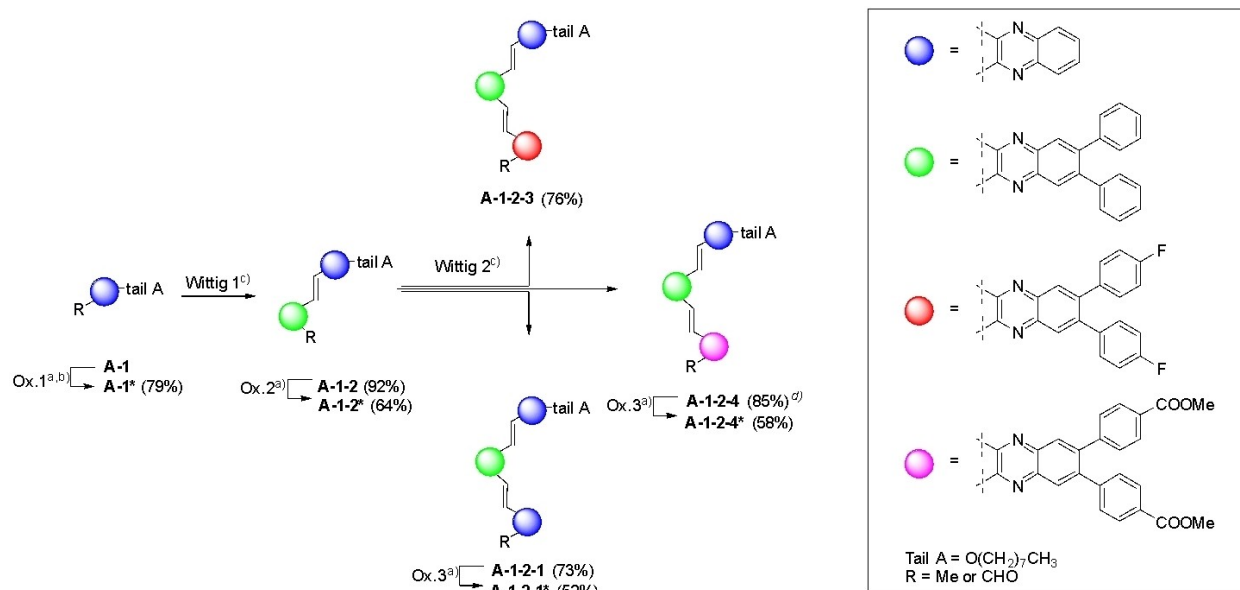
Discussion

To investigate the photophysical properties of the obtained compounds, the quantitative UV-Vis absorption spectra of the different monomers and oligomers were measured in dichloromethane and at a concentration of 18 μM (Figure 3).

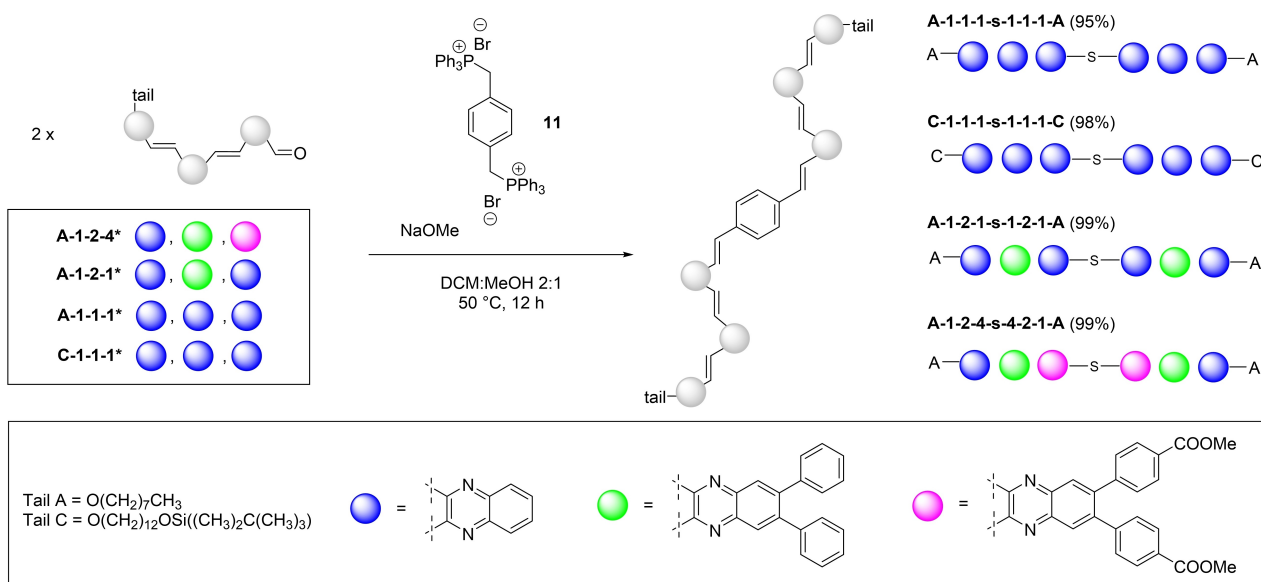
As shown in the UV-Vis absorption spectra of **B-1-1** and **B-1-1*** (Figure 3a), oxidation of the terminal methyl group has only a minor influence on the absorption properties of the oligomers. Light absorption at the global maximum decreases slightly; however, the wavelength remains almost unchanged with $\lambda_{\text{max}} = 389 \text{ nm}$ (**B-1-1**) and $\lambda_{\text{max}} = 386 \text{ nm}$ (**B-1-1***). Further, UV-Vis spectra of oxidized oligomers have not been measured due to the lower stability of the aldehydes concerning the methyl derivatives.

A stepwise extension of the π system in **A-1** to **A-1-1-1-s-1-1-1-A** affects the light absorption properties of the respective oligomers, as shown in Figure 3b. With each additional building block, absorption shifts more from the UV to the visible region of the light spectrum. A large difference from **A-1** to **A-1-1** regarding absorption area can be observed, while this difference is less pronounced concerning larger oligomers **A-1-1-1** and **A-1-1-1-s-1-1-1-A**. In the case of **A-1-1-1**, the absorption maxima are less specific: Whereas **A-1-1** shows one distinct maximum at $\lambda_{\text{max}} = 392 \text{ nm}$, **A-1-1-1** exhibits an almost constant light absorption between $\lambda = 320 \text{ nm}$ and $\lambda = 410 \text{ nm}$. In the dimerized oligomer **A-1-1-1-s-1-1-1-A**, light absorption is substantially increased compared to the non-dimerized oligomers, and other specific absorption bands are visible at $\lambda_{\text{max}} = 321 \text{ nm}$ and $\lambda_{\text{max}} = 398 \text{ nm}$.

Similar to the case of the terminal methyl group, alteration of the tail structure has no significant influence on the UV-Vis absorption profile of the trimers (**A/B/C/D-1-1-1**, see Supporting



Scheme 4. Schematic representation of the oligomer syntheses. [a] Conditions: SeO_2 (2.0 to 5.0 equiv.), 1,4-dioxane, 50 °C to 80 °C, 12 h; [b] TBHP (1.1 equiv.); [c] Conditions: phosphonium salt 1–4 (1.1 to 1.5 equiv.), NaOMe (5.0 equiv.), DCM:MeOH (2:1), 50 °C, 12 h. [d] reaction was conducted at 21 °C instead of 50 °C.



Scheme 5. Coupling between different oligomers with linking agent **11** using Wittig reaction. Conditions: NaOMe (5.0 equiv.), DCM:MeOH 2:1, 50 °C, 12 h. Conditions: NaOMe (5.0 equiv.), DCM:MeOH 2:1, 50 °C, 12 h. Explanation: s = spacer/linking unit.

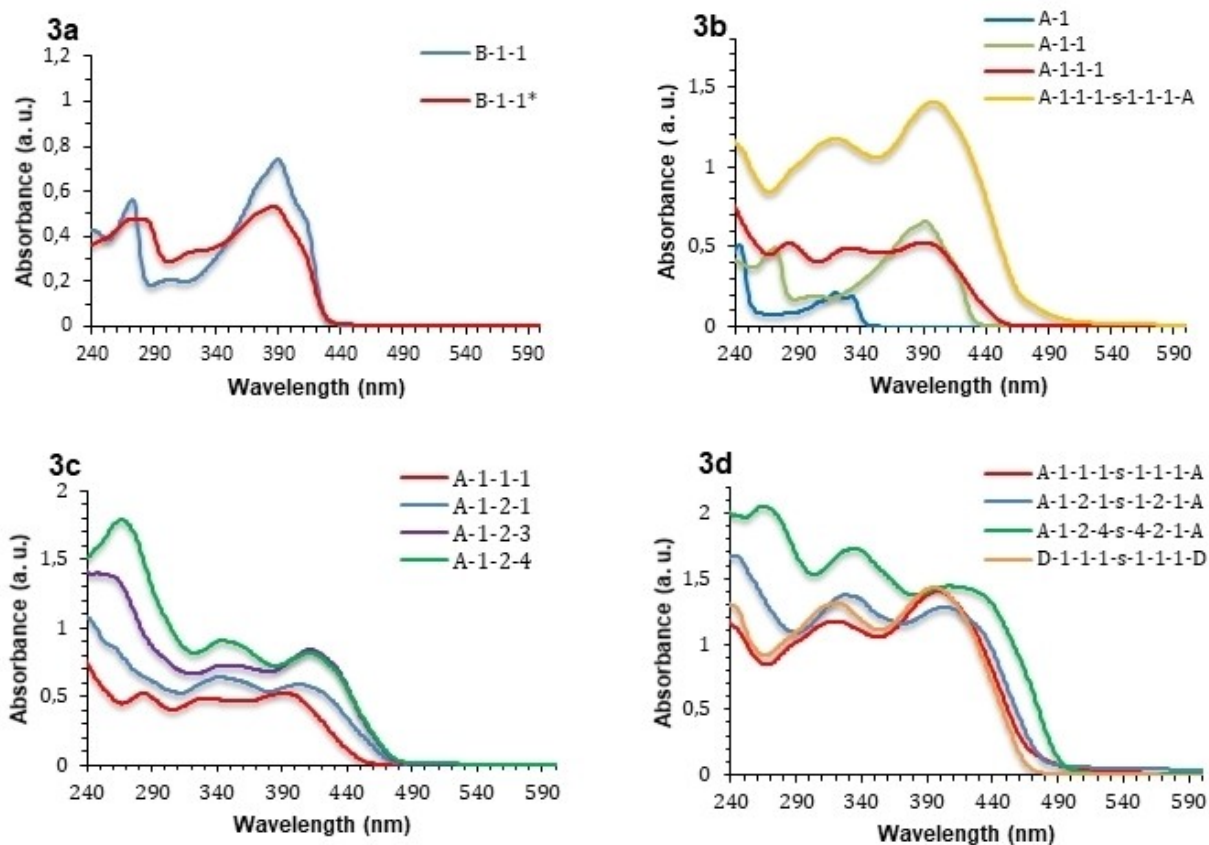


Figure 3. Quantitative UV-Vis absorption spectra of the oxidized **B-1-1*** and non-oxidized **B-1-1** (Figure 3a) of oligomers with increasing length **A-1** to **A-1-1-1-s-1-1-1-A** (Figure 3b), of various trimers **A-X-X-X** (Figure 3c) and the 3 + 3 oligomers **A/D-1/2-1/4-s-1/4-1/2-1-A/D** (Figure 3d). UV-Vis spectra were recorded in dichloromethane at 18 μ M.

Information Figure S2). Modifications to the quinoxalines' backbone provoke absorption changes consistent with the expect-

tions that electronic changes alter the molecules' properties, as shown in Figure 3c. Compared to the compound with an

unsubstituted backbone (A-1-1-1), all backbone-modified oligomers showed a slight redshift of the absorption spectra. Electron withdrawing substituents (A-1-2-3 and A-1-2-4) gave a slightly higher redshift compared to A-1-1-1 than A-1-2-1 compared to A-1-1-1.

The 3+3 oligomers tend to have two specific absorption maxima each, even though light absorption is generally throughout the entire UV window. It can also be noted that the light absorption of these oligomers stretches further into the visible region than in the tail-X-X oligomers, with A-1-2-4-s-4-2-1-A reaching up to $\lambda = 500$ nm (see Figure 3d).

Quantitative UV-Vis emission spectra of various compounds with the structure tail-X-X and dimerized 3+3 oligomers were recorded under the same conditions as their absorption spectra (Figure 4). The measurements were conducted with an excitation wavelength derived from previously recorded excitation-emission matrices (EEM; see Figure S3).

The observations from the emission spectra are consistent with the findings in light absorption behavior: by modifying the electron properties of the oligomer with a tuned backbone, a slight shift of emission towards the visible region can be noted ($\lambda_{\text{max}} = 455$ nm (A-1-1-1), $\lambda_{\text{max}} = 480$ nm, (A-1-2-4)). Generally, light emission intensity is substantially higher in oligomers such as A-1-2-4 (intensity_{max} = 3518 i. u.), with modifications on the quinoxaline backbone, compared to unsubstituted analogs like A-1-1-1 (intensity_{max} = 1655 i. u.).

The same applies to dimerized 3+3 oligomers. In this case, alterations at the tail region do not influence the emission profile of the oligomers (A-1-1-1-s-1-1-1-A and D-1-1-1-s-1-1-1-D). Extension of the π -system instead increases the emission intensity and shifts the emission maximum towards higher wavelengths. Moreover, an observation can be made regarding the shape of the emission curve: Regarding the 3+3 oligomers, the emission properties are more specific than trimers. One prominent emission maximum and a second one can be seen for trimers, whereas only one maximum is visible in the emission spectra of 3+3 oligomers. An exception from this, however, is observed for A-1-2-1-s-1-2-A.

Conclusion

A new process for synthesizing tunable oligomers based on quinoxaline units was elaborated and optimized using Wittig coupling. This new synthesis route offers much diversity regarding the accessible oligomers. The elaborated two-step oligomerization process, containing repetitive sequences of selective oxidations and Wittig coupling reactions, ensured the selective assembly of quinoxaline-based monomers to form various oligomers up to 3+3 units and 4 units. The quinoxaline monomers could be functionalized on the benzene ring with various substituents, whereas the pyrazine ring served for chain extension. Variations in the tail region could improve the solubility properties of the oligomers or provide enhanced purification options. Some tail structures (perfluorinated and non-perfluorinated) were also used to increase and promote chemical properties enabling the oligomer-building process, thus achieving the 4 unit oligomer. Some easy-to-access quinoxaline-based triphenylphosphonium salts were synthesized, bearing differently substituted backbones to realize such coupling. Finally, the optical properties of the obtained oligomers were examined. The 3+3 oligomers were shown to possess fluorescent properties ranging from moderate to good (especially the oligomer A-1-2-4-s-4-2-1-A). The emission intensity strongly depends on the oligomer's modifications of the quinoxaline backbone and the size of the oligomer.

Experimental Section

Exemplarily selected experiments describing the main steps in the process described in this manuscript.

2-(Bromomethyl)-3-methylquinoxaline (10a)

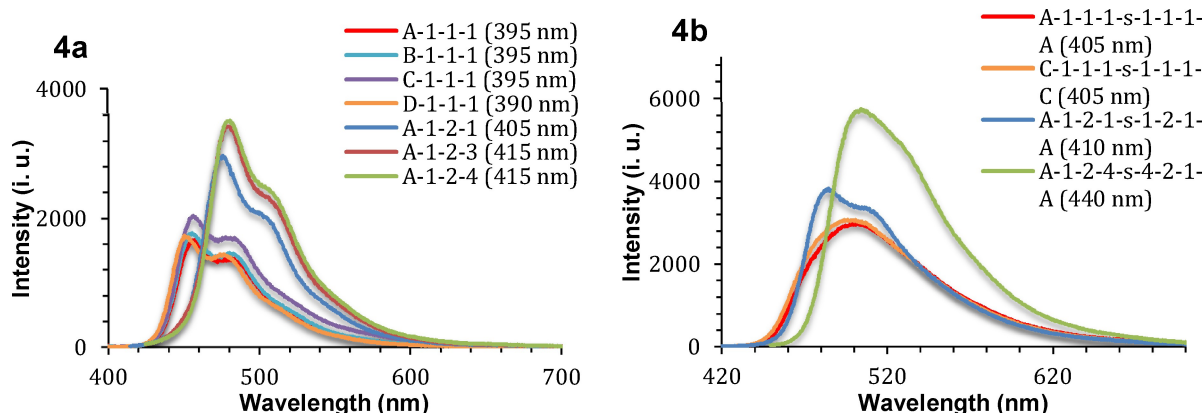
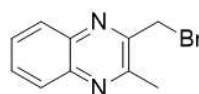
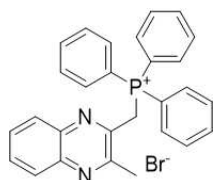


Figure 4. Quantitative UV-Vis emission spectra of tail-1-1-2/1-3/4 (Figure 4a) and the coupled oligomers A/D-1-2-1/4-s-1/4-1/2-1-A/D (Figure 4b). Spectra were recorded in dichloromethane at 18 μM using an excitation wavelength derived from previously recorded Excitation-Emission Matrices (EEM); see Figure S3.

2,3-Dimethylquinoxaline (3.60 g, 23 mmol, 1.00 equiv.), 1-bromopyrrolidine-2,5-dione (3.65 g, 20 mmol, 0.900 equiv.) and benzoyl benzenecarboperoxoate (441 mg, 1.37 mmol, 0.0600 equiv) were dissolved in acetonitrile (180.00 mL) and heated to 95 °C for 4 h. 1-Bromopyrrolidine-2,5-dione (2.03 g, 11 mmol, 0.500 equiv.) and benzoyl benzenecarboperoxoate (441 mg, 1.37 mmol, 0.0600 equiv.) were added again and the reaction was heated to 95 °C for 2 h. Then benzoyl benzenecarboperoxoate (220 mg, 683 μmol, 0.0300 equiv.) and 1-bromopyrrolidine-2,5-dione (810 mg, 4.55 mmol, 0.200 equiv.) were added again and the reaction was heated to 95 °C for 1 h. The reaction was allowed to reach 21 °C. Methylene chloride (1000 mL) and distilled water (1000 mL) were then added and the aqueous layer was extracted 3x with methylene chloride (500 mL each time). The organic layers were combined and dried over Na₂SO₄. The solvent was removed under reduced pressure. The obtained crude product was purified via flash-chromatography on silica gel using cyclohexane/ethyl acetate 1:0 to 20:1 to afford 2-(bromomethyl)-3-methylquinoxaline (3.76 g, 15.9 mmol, 70% yield) as a colorless solid. *R*_f = 0.51 (cyclohexane/ethyl acetate 4:1). ¹H NMR (400 MHz, CDCl₃, ppm) δ = 2.88 (s, 3H, CH₃), 4.75 (s, 2H, CH₂), 7.60–7.84 (m, 2H, H_{Ar}), 7.94–8.11 (m, 2H, H_{Ar}); ¹³C NMR (100 MHz, CDCl₃, ppm) δ = 22.5, 31.9, 128.5, 129.1, 129.6, 130.6, 141.0, 142.0, 151.0, 153.2; IR (ATR, $\tilde{\nu}$) = 3054, 3024, 2968, 2918, 2883, 2857, 2435, 2115, 1962, 1942, 1912, 1851, 1827, 1778, 1720, 1635, 1604, 1582, 1561, 1485, 1465, 1442, 1426, 1392, 1371, 1354, 1320, 1292, 1272, 1259, 1214, 1180, 1123, 1103, 1069, 1026, 1003, 984, 959, 924, 892, 874, 813, 765, 730, 714, 686, 674, 652, 609, 595, 565, 527, 517, 490, 477, 422, 388, 378 cm⁻¹; EI (*m/z*, 70 eV, 20 °C): 238/236 (19/18) [M]⁺, 158 (12), 157 (100), 89 (15), 76 (13). HRMS-EI (*m/z*): [M]⁺ calcd for C₁₀H₉N₂⁷⁹Br₁, 235.9949; found 235.9949.

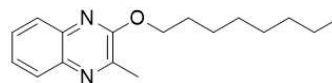
((3-Methylquinoxalin-2-yl)methyl)triphenylphosphonium bromide (1)



Triphenylphosphane (4.98 g, 19.0 mmol, 5.00 equiv.) was put under N₂ and dry methylene chloride (20.0 mL) was added. The solution was cooled to -78 °C and 2-(bromomethyl)-3-methylquinoxaline (900 mg, 3.80 mmol, 1.00 equiv.) in methylene chloride (15.0 mL) was added dropwise under strong agitation. The solution was stirred for 1 h at -78 °C and the solution was allowed to reach 21 °C during 12 h. The obtained crude product was purified via flash-chromatography on silica gel using methylene chloride/methanol 10:1 to afford ((3-methylquinoxalin-2-yl)methyl)triphenylphosphonium bromide (1.39 g, 2.78 mmol, 73% yield) as a beige solid. *R*_f = 0.19 (methylene chloride/methanol 20:1). ¹H NMR (400 MHz, CDCl₃, ppm) δ = 3.09 (s, 3H, CH₃), 6.21 (d, ¹J_{HP} = 13.3 Hz, 2H, CH₂), 7.36 (dd, *J* = 8.3 Hz, *J* = 1.3 Hz, 1H, H_{Ar}), 7.52 (ddd, *J* = 8.3 Hz, *J* = 6.9 Hz, *J* = 1.4 Hz, 1H, H_{Ar}), 7.56–7.63 (m, 6H, H_{Ar}), 7.63–7.73 (m, 4H, H_{Ar}), 7.89–8.05 (m, 7H, H_{Ar}); ¹³C NMR (100 MHz, CDCl₃, ppm) δ = 24.0, 33.1 (d, ¹J_{CP} = 58.5 Hz, CH₂), 119.9 (d, ¹J_{CP} = 89.4 Hz, 3 C, C'), 127.1, 128.6, 129.5, 130.1 (d, ²J_{CP} = 13.0 Hz, 6 C, C'), 130.3, 134.2 (d, ³J_{CP} = 10.4 Hz, 6 C, C''), 134.5 (d, ⁴J_{CP} = 3.1 Hz, 3 C, C'''), 139.1 (2 C), 146.9 (d, ²J_{CP} = 7.0 Hz), 154.6 (d, ³J_{CP} = 8.3 Hz); IR (ATR, $\tilde{\nu}$) = 3092, 3051, 3006, 2986, 2965, 2908, 2803, 2745, 2234, 2164, 2055, 1972, 1907, 1819, 1778, 1717, 1684, 1647, 1609, 1585, 1567, 1483, 1435, 1397, 1377, 1354, 1333, 1315, 1288, 1262, 1238, 1203, 1183, 1159, 1137, 1106, 1098, 1024, 1007, 996, 958, 931, 911, 897,

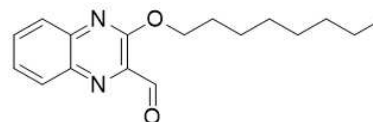
873, 857, 809, 793, 765, 749, 734, 722, 713, 688, 612, 552, 513, 504, 490, 475, 448, 425, 409, 392, 380 cm⁻¹; EI (*m/z*, 70 eV, 20 °C): 420 (32) [M–Br+H]⁺, 419 [M–Br]⁺ (100). HRMS-EI (*m/z*): [M]⁺ calcd for C₂₈H₂₃N₂⁷⁹Br₁P₁, 497.0782; found, 497.0783.

2-Methyl-3-(octyloxy)quinoxaline (A-1)



To a solution of dry N,N-dimethylformamide (3.00 mL) and octan-1-ol (80.2 mg, 97.7 μL, 616 μmol, 1.10 equiv.), potassium hydroxide (37.7 mg, 672 μmol, 1.20 equiv.) was added under N₂ atmosphere. Then 2-chloro-3-methylquinoxaline (100 mg, 560 μmol, 1.00 equiv.) was added. The mixture was stirred at 21 °C for 12 h. Then ethyl acetate (20 mL) and distilled water (20 mL) were added. The organic layer was washed 3 × (10 mL each time) with dist. water. The remaining aqueous layer was extracted 1 × (10 mL) with ethyl acetate. The combined organic layer was dried over Na₂SO₄, filtered and the solvent was removed under reduced pressure. The obtained crude product was purified via flash-chromatography on silica gel using cyclohexane/ethyl acetate 1:0 to 20:1 to afford 2-methyl-3-(octyloxy)quinoxaline (135 mg, 496 μmol, 89% yield) as a colorless solid. *R*_f = 0.24 (cyclohexane/ethyl acetate 4:1). ¹H NMR (400 MHz, CDCl₃, ppm) δ = 0.77–0.95 (m, 3H, CH₃CH₂), 1.16–1.42 (m, 8H, CH₂), 1.43–1.56 (m, 2H, CH₂), 1.84 (p, *J* = 6.8 Hz, 2H, CH₂CH₂O), 2.62 (s, 3H, CH₃), 4.46 (t, *J* = 6.6 Hz, 2H, CH₂O), 7.49 (ddd, *J* = 8.3 Hz, *J* = 7.0 Hz, *J* = 1.5 Hz, 1H, H_{Ar}), 7.56 (ddd, *J* = 8.3 Hz, *J* = 7.0 Hz, *J* = 1.6 Hz, 1H, H_{Ar}), 7.77 (dd, *J* = 8.2 Hz, *J* = 1.5 Hz, 1H, H_{Ar}), 7.91 (dd, *J* = 8.2 Hz, *J* = 1.5 Hz, 1H, H_{Ar}); ¹³C NMR (100 MHz, CDCl₃, ppm) δ = 14.2 (CH₃), 20.5 (CH₃), 22.8 (CH₂), 26.3 (CH₂), 28.9 (CH₂), 29.4 (CH₂), 29.5 (CH₂), 31.9 (CH₂), 66.7 (CH₂), 126.2 (CH), 126.8 (CH), 128.1 (CH), 128.8 (CH), 138.5 (Cq), 140.1 (Cq), 148.4 (Cq), 156.6 (Cq); IR (ATR, $\tilde{\nu}$) = 3058, 2953, 2924, 2850, 1604, 1581, 1497, 1460, 1424, 1385, 1374, 1358, 1323, 1286, 1251, 1225, 1183, 1139, 1120, 1082, 1061, 1038, 1023, 1006, 989, 972, 959, 926, 895, 875, 864, 789, 759, 738, 718, 676, 608 cm⁻¹; UV-VIS (absorption, CH₂Cl₂ [18 μmol/L], 21 °C), λ_{max} (log ε in M⁻¹cm⁻¹) = 333 (4.02), 320 (4.07), 244 (4.45) nm; EI (*m/z*, 70 eV, 30 °C): 272 (22) [M]⁺, 257 (10), 161 (19), 160 (100), 143 (10), 132 (53), 131 (13), 90 (12). HRMS-EI (*m/z*): [M]⁺ calcd for C₁₇H₂₄O₁N₂, 272.1883; found, 272.1882.

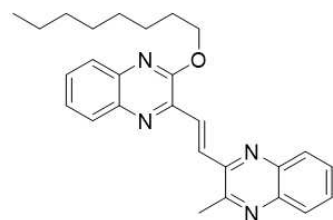
3-(Octyloxy)quinoxaline-2-carbaldehyde (A-1*)



Selenium dioxide (2.04 g, 18.4 mmol, 5.00 equiv.) and 2-methyl-3-(octyloxy)quinoxaline (1.00 g, 3.67 mmol, 1.00 equiv.) were dissolved in 1,4-dioxane (20.00 mL) and then tert-butyl hydroperoxide (1.04 g, 1.47 mL, 8.08 mmol, 5.50 M, 2.20 equiv.) in decane was added. The solution was stirred to 50 °C for 12 h. The solution was allowed to reach 21 °C. Methylene chloride (250 mL) and distilled water (200 mL) were then added and the aqueous layer was extracted 3x with methylene chloride (100 mL) each time. The organic layers were combined and dried over Na₂SO₄. The solvent was removed under reduced pressure. The obtained crude product was purified via flash-chromatography on silica gel using cyclohexane/ethyl acetate 1:0 to 4:1 to afford 3-(octyloxy)quinoxaline-2-carbaldehyde (835 mg, 2.92 mmol, 79% yield) as a beige solid. *R*_f = 0.61 (cyclohexane/ethyl acetate 4:1). ¹H

NMR (400 MHz, CDCl₃ [7.27 ppm], ppm) δ = 0.83–0.93 (m, 3H, CH₂CH₃), 1.21–1.45 (m, 8H, CH₂), 1.46–1.58 (m, 2H, CH₂), 1.85–1.96 (m, 2H, CH₂), 4.59 (t, *J* = 6.7 Hz, 2H, OCH₂), 7.54–7.69 (m, 1H, H_{Ar}), 7.72–7.83 (m, 1H, H_{Ar}), 7.83–7.88 (m, 1H, H_{Ar}), 8.08–8.22 (m, 1H, H_{Ar}), 10.44 (s, 1H, CHO); ¹³C NMR (100 MHz, CDCl₃ [77.0 ppm], ppm) δ = 14.2 (CH₃), 22.8 (CH₂), 26.2 (CH₂), 28.8 (CH₂), 29.3 (CH₂), 29.4 (CH₂), 31.9 (CH₂), 67.4 (CH₂), 127.2 (CH), 127.7 (CH), 130.6 (CH), 133.2 (CH), 138.7 (Cq), 138.8 (Cq), 142.5 (Cq), 157.3 (Cq), 189.7 (CHO); IR (ATR, $\tilde{\nu}$) = 2959, 2915, 2897, 2867, 2849, 2812, 2768, 2730, 2701, 1721, 1684, 1609, 1557, 1493, 1466, 1414, 1377, 1343, 1323, 1298, 1258, 1224, 1190, 1156, 1139, 1120, 1078, 1060, 1038, 1021, 979, 943, 929, 904, 891, 875, 853, 793, 764, 737, 720, 637, 620, 605, 557, 543, 521, 496, 472, 442, 392, 385 cm⁻¹; UV-VIS (absorption, CH₂Cl₂), λ_{max} = 360, 308, 254 nm; MS (ESI), *m/z* (%): 288 (18) [M + 2H]⁺, 287 (100) [M + H]⁺. HRMS-ESI (*m/z*): [M + H]⁺ calcd for C₁₇H₂₃N₂O₂ 287.1681; found 287.1751.

(E)-2-Methyl-3-(2-(3-(octyloxy)quinoxalin-2-yl)vinyl)quinoxaline (A-1-1)



3-(Octyloxy)quinoxaline-2-carbaldehyde (630 mg, 2.20 mmol, 1.00 equiv.), ((3-methylquinoxalin-2-yl)methyl)triphenylphosphonium bromide (1.21 g, 2.42 mmol, 1.10 equiv.) and sodium methoxide (594 mg, 11.0 mmol, 5.00 equiv.) were put under argon. Then dry methanol (7.0 mL) and dry methylene chloride (14.0 mL) were added and the reaction was heated to 50 °C for 12 h. Methylene chloride (250 mL) was added. The organic layer was washed with brine (200 mL). Then the aqueous layer was extracted three times with methylene chloride (250 mL each time). The organic layers were combined, dried over Na₂SO₄ and filtered. The solvent was removed under reduced pressure. The obtained crude product was purified via flash-chromatography on silica gel using cyclohexane/ethyl acetate 1:0 to 10:1 to afford (E)-2-methyl-3-(2-(3-(octyloxy)quinoxalin-2-yl)vinyl)quinoxaline (829 mg, 1.94 mmol, 88% yield) as a yellow solid. *R_f* = 0.53 (cyclohexane/ethyl acetate 4:1). ¹H NMR (400 MHz, CDCl₃ [7.27 ppm], ppm) δ = 0.81–0.93 (m, 3H, CH₂CH₃), 1.2–1.49 (m, 8H, CH₂), 1.52–1.64 (m, 2H, CH₂), 1.91–2.02 (m, 2H, CH₂), 2.98 (s, 3H, CH₃), 4.59 (t, *J* = 6.7 Hz, 2H, OCH₂), 7.56 (ddd, *J* = 8.3 Hz, *J* = 7.0 Hz, *J* = 1.5 Hz, 1H, H_{Ar}), 7.64 (ddd, *J* = 8.4 Hz, *J* = 7.0 Hz, *J* = 1.5 Hz, 1H, H_{Ar}), 7.68–7.76 (m, 2H, H_{Ar}), 7.81 (dd, *J* = 8.4 Hz, *J* = 1.2 Hz, 1H, H_{Ar}), 7.98–8.03 (m, 1H, H_{Ar}), 8.04 (dd, *J* = 8.4 Hz, *J* = 1.4 Hz, 1H, H_{Ar}), 8.08–8.15 (m, 1H, H_{Ar}), 8.42 (d, *J* = 15.4 Hz, 1H, H_{Alkene}), 8.47 (d, *J* = 15.4 Hz, 1H, H_{Alkene}); ¹³C NMR (100 MHz, CDCl₃ [77.0 ppm], ppm) δ = 14.2 (CH₃), 22.8 (CH₂), 23.1 (CH₃), 26.4 (CH₂), 29.0 (CH₂), 29.4 (CH₂), 29.5 (CH₂), 32.0 (CH₂), 67.2 (CH₂), 126.9 (2 C, CH), 128.3 (CH), 129.1 (CH), 129.4 (CH), 129.6 (CH), 130.0 (CH), 130.1 (CH), 130.6 (CH), 130.8 (CH), 139.1 (Cq), 140.7 (Cq), 141.6 (Cq), 141.7 (Cq), 143.2 (Cq), 149.4 (Cq), 153.2 (Cq), 156.3 (Cq); IR (ATR, $\tilde{\nu}$) = 3061, 2952, 2919, 2893, 2871, 2851, 1625, 1609, 1571, 1553, 1489, 1466, 1434, 1415, 1391, 1371, 1364, 1346, 1332, 1312, 1281, 1272, 1230, 1218, 1207, 1149, 1136, 1126, 1108, 1082, 1064, 1026, 1016, 1006, 976, 960, 950, 924, 909, 870, 860, 802, 789, 765, 755, 722, 703, 683, 630, 606, 560, 547, 531, 523, 490, 477, 443, 426, 404, 390 cm⁻¹; UV-VIS (absorption, CH₂Cl₂ [18 μ mol/L], 21 °C), λ_{max} (log ϵ in M⁻¹cm⁻¹) = 392 (4.56), 272 (4.44) nm; MS (ESI), *m/z* (%): 428 (26) [M + 2H]⁺, 427 (100) [M + H]⁺, 297 (32), 282 (71), 223

(91). HRMS-ESI (*m/z*): [M + H]⁺ calcd for C₂₇H₃₁N₄O 427.2419; found 427.2489.

Funding

This project has been funded by the German Research Foundation (DFG grants BR 1750/50-1 and JU 1352/6-1, project number: 367274963).

Acknowledgements

We thank Victor Larignon for assisting the project during his internship and Christoph W. Grathwol for improving the publication. We thank Frank Kirschhöfer and Henry Unger for measuring oligomers' masses on a MALDI-TOF device and André Jung and Laura Holzhauer for their support regarding the UV-Vis and fluorescence measurements. We thank the KIT Soft Matter Synthesis Laboratory for the opportunity to use their UV-Vis spectrophotometer. This work was supported by the Helmholtz research area Information and benefitted from the work of the DFG core facility Molecule Archive. Open Access funding enabled and organized by Projekt DEAL.

Conflict of Interest

The authors declare no conflict of interest.

Data Availability Statement

The Supplemental Information covers detailed material on the conducted experiments and their results. All experimental details, including the analytical description of the obtained target compounds, are available in Supplemental Information Part 1. Information on the data's availability and the target compounds' physical material is added to Supplemental Information Part 2. Data that refers to the herein described experiments were submitted to the repository chemotion (<https://www.chemotion-repository.net/>). New data obtained in this study is assigned to the collection embargo number JPK_2020-03-10.^[25]

Keywords: oligomerization · perfluoro chain · quinoxaline · Wittig reaction · synthetic methods

- [1] G. Yashwantrao, S. Saha, *Org. Chem. Front.* **2021**, *8*, 2820–2862.
- [2] L. E. Seitz, W. J. Suling, R. C. Reynolds, *J. Med. Chem.* **2002**, *45*, 5604–5606.
- [3] S. Y. Hassan, S. N. Khattab, A. A. Bekhit, A. Amer, *Bioorg. Med. Chem. Lett.* **2006**, *16*, 1753–1756.
- [4] F. Rong, S. Chow, S. Yan, G. Larson, Z. Hong, J. Wu, *Bioorg. Med. Chem. Lett.* **2007**, *17*, 1663–1666.
- [5] M. Tristan-Manzano, A. Guirado, M. Martinez-Esparza, J. Galvez, P. Garcia-Penarrubia, J. A. Ruiz-Alcaraz, *Curr. Med. Chem.* **2015**, *22*, 3075–3108.

- [6] Y. Ramli, A. Moussaif, K. Karrouchi, E. M. Essassi, *J. Chem.* **2014**, *2014*, 563406.
- [7] J. Yuan, J. Ouyang, V. Cimrová, M. Leclerc, A. Najari, Y. Zou, *J. Mater. Chem. C* **2017**, *5*, 1858–1879.
- [8] J. Li, J. Miao, G. Long, J. Zhang, Y. Li, R. Ganguly, Y. Zhao, Y. Liu, B. Liu, Q. Zhang, *J. Mater. Chem. C* **2015**, *3*, 9877–9884.
- [9] E. Wang, L. Hou, Z. Wang, S. Hellström, F. Zhang, O. Inganäs, M. R. Andersson, *Adv. Mater.* **2010**, *22*, 5240–5244.
- [10] Y. Hanyu, T. Sugimoto, Y. Ganbe, A. Masuda, I. Honma, *J. Electrochem. Soc.* **2013**, *161*, A6–A9.
- [11] R. Sim, W. Ming, Y. Setiawan, P. S. Lee, *J. Phys. Chem. C* **2013**, *117*, 677–682.
- [12] Y. Ito, T. Miyake, S. Hatano, R. Shima, T. Ohara, M. Sugimoto, *J. Am. Chem. Soc.* **1998**, *120*, 11880–11893.
- [13] M. Sugimoto, T. Yamamoto, Y. Nagata, *J. Synth. Org. Chem. Jpn.* **2015**, *73*, 1141–1155.
- [14] Y. Ito, E. Ihara, M. Hirai, H. Ohsaki, A. Ohnishi, M. Murakami, *J. Chem. Soc. Chem. Commun.* **1990**, 403–405.
- [15] Y.-X. Xue, Y.-Y. Zhu, L.-M. Gao, X.-Y. He, N. Liu, W.-Y. Zhang, J. Yin, Y. Ding, H. Zhou, Z.-Q. Wu, *J. Am. Chem. Soc.* **2014**, *136*, 4706–4713.
- [16] Y. Ito, T. Ohara, R. Shima, M. Sugimoto, *J. Am. Chem. Soc.* **1996**, *118*, 9188–9189.
- [17] C. Xu, C. He, N. Li, S. Yang, Y. Du, K. Matyjaszewski, X. Pan, *Nat. Commun.* **2021**, *12*, 5853.
- [18] G. Y. Krippner, M. M. Harding, *Tetrahedron: Asymmetry* **1994**, *5*, 1793–1804.
- [19] S. Karpagam, S. Guhanathan, P. Sakthivel, *Fibers Polym.* **2012**, *13*, 1105–1112.
- [20] A. Upadhyay, S. Karpagam, *Dyes Pigm.* **2017**, *139*, 50–64.
- [21] W. Zhang, D. P. Curran, *Tetrahedron* **2006**, *62*, 11837–11865.
- [22] K. Y. Yoshinobu Tagawa, Y. Higuchi, Y. Goto, *Heterocycles* **2003**, *60*, 953–957.
- [23] H. Sakai, S. Shinto, Y. Araki, T. Wada, T. Sakanoue, T. Takenobu, T. Hasobe, *Chem. Eur. J.* **2014**, *20*, 10099–10109.
- [24] S. Shrestha, B. R. Bhattarai, B. Kafle, K.-H. Lee, H. Cho, *Bioorg. Med. Chem.* **2008**, *16*, 8643–8652.
- [25] The data of this study is available as Open Access in the repository chemotion: It can be accessed either by following the DOI-links in the Supplemental Information or via the publications list on <https://www.chemotion-repository.net/> and filtering with the embargo number JPK_2020-03-10.

Manuscript received: November 24, 2022
Revised manuscript received: December 10, 2022